

Raman coupler for a trapped two-component quantum-degenerate Fermi gas

Sierk Pötting^{1,2,3}, Marcus Cramer^{1,4}, Weiping Zhang¹, and Pierre Meystre¹

¹*Optical Sciences Center, The University of Arizona, Tucson, AZ 85721*

²*Max-Planck-Institut für Quantenoptik, 85748 Garching, Germany*

³*Sektion Physik, Universität München, 80333 München, Germany*

⁴*Fachbereich Physik der Philipps-Universität, 35032 Marburg, Germany*

(Dated: December 2, 2024)

We investigate theoretically the Raman coupling between two internal states of a trapped low-density quantum-degenerate Fermi gas. In general, the trap frequencies associated with the two internal states can be different, leading to the onset of collapses and revivals in the population difference ΔN of the two internal states. This behavior can be changed drastically by two-body collisions. In particular, we show that under appropriate conditions they can suppress the dephasing leading to the collapse of ΔN , and restore almost full Rabi oscillations between the two internal states. These results are compared and contrasted to those for a quantum-degenerate bosonic gas.

PACS numbers: 03.75.Fi, 75.45.+j, 75.60.Ej

I. INTRODUCTION

Quantum-degenerate samples of low-density fermionic atomic gases [1, 2] are arguably even more interesting than their bosonic counterparts [3], due to the fundamental role played by the Pauli exclusion principle in their dynamics. This principle renders their experimental realization particularly difficult, since in the simplest case, the collisions that are essential in evaporative cooling largely disappear as the temperature of the sample goes to zero. For this reason, more elaborate techniques, involving e.g. the use of several isotopes, or sympathetic cooling via a bosonic system, have been used to achieve degeneracy [1]. Collisions also leave behind holes in the Fermi sea[4]; these holes are difficult to fill and are believed to limit the temperatures that can be achieved in practice to about $0.2 T_F$, where T_F is the Fermi temperature.

From a theoretical viewpoint, Fermi systems also present a number of difficult challenges. In particular, they are not amenable to a mean-field description. Hence they cannot be analyzed in a classical-like formalism such as the Gross-Pitaevskii equation, which has proven remarkably powerful in describing many aspects of quantum-degenerate bosonic systems. On the other hand, the additional complexity of Fermi systems also offers much promise. One can hope to be able to manipulate them into strongly non-classical states, with potential applications in atom interferometry. Also, the nonlinear mixing of fermionic matter waves is expected to be very different from the bosonic case. As such, Fermi systems promise the extension of nonlinear atom optics[5] to a regime without counterpart in traditional nonlinear optics.

Just as is the case for bosons, a cornerstone of the manipulation of fermionic matter waves is their interaction with light. In this paper, we discuss the specific situation where transitions between two internal states of a trapped quantum-degenerate Fermi system at zero temperature are induced by Raman coupling. A straight-

forward generalization of this model could be used to describe an output coupler for an atom laser [6]. Our goal is two-fold: first, to understand the difference between the bosonic and fermionic dynamics; and second, to determine the role of two-body collisions on the evolution of the system.

We first consider the dynamics of the system in the absence of collisions. Section II introduces our model and derives the Heisenberg equations of motion for the relevant atomic fields, and section III compares the resulting dynamics with those for a corresponding Bose gas. Collisions are introduced in section IV. The resulting equations of motion are solved numerically in the framework of a time-dependent Hartree-Fock theory for the case of fermions, and in a standard mean-field theory for a bosonic sample. Again, we give a detailed comparison of the two situations, and illustrate how collisions can change the fermionic dynamics in a non-trivial fashion. Finally, Section V is a summary and conclusion.

II. MODEL

We consider a two-component quantum-degenerate atomic system trapped in a one-dimensional, harmonic potential with each component corresponding, e.g., to one internal hyperfine spin state. In general, the coupling of the atoms to the trapping field is different for the two (spin) components $|+\rangle$ and $|-\rangle$, so that they see trapping potentials of different frequencies ω_+ and ω_- . The two internal states are coupled by a Raman-type interaction of frequency ν equal to the spin-flip transition frequency of the atoms in the ground state of the two trapping potentials. This model, which is summarized on the diagram of Fig. 1, is described by the second-quantized Hamiltonian

$$\hat{\mathcal{H}} = \int dx \hat{\Psi}_+^\dagger(x) H_+ \hat{\Psi}_+(x) + \int dx \hat{\Psi}_-^\dagger(x) H_- \hat{\Psi}_-(x)$$

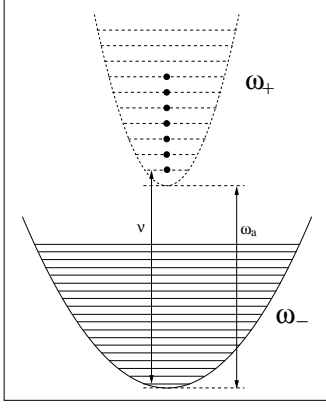


FIG. 1: Two-component Fermi gas in a harmonic trap. The trapping frequencies ω_+ and ω_- correspond to the two internal states, which are coupled via a spin-flip transition at frequency ν resonant with the frequency difference of the trap ground states.

$$+ \hbar g \int dx \left[e^{-i\nu t} \hat{\Psi}_+^\dagger(x) \hat{\Psi}_-(x) + h.c. \right], \quad (1)$$

where $\hbar g$ is the Raman coupling strength. The first-quantized Hamiltonian describing the trapping potentials associated with the internal states $|+\rangle$ and $|-\rangle$ are

$$H_\pm = -\frac{\hbar^2}{2m} \frac{\partial^2}{\partial x^2} + \frac{1}{2} m \omega_\pm^2 x^2 + E_\pm, \quad (2)$$

with E_\pm being the energy of the internal state $|\pm\rangle$. The Raman resonance condition is therefore, with $\omega_a = \omega_+ - \omega_-$,

$$\nu = \omega_a + (\omega_+ - \omega_-)/2. \quad (3)$$

The atomic field operators corresponding to the two traps obey the fermionic, respectively bosonic (anti)commutation relations

$$\begin{aligned} \left[\hat{\Psi}_i(x), \hat{\Psi}_j^\dagger(x') \right]_\pm &= \delta_{ij} \delta(x - x'), \\ \left[\hat{\Psi}_i(x), \hat{\Psi}_j(x') \right]_\pm &= 0, \\ \left[\hat{\Psi}_i^\dagger(x), \hat{\Psi}_j^\dagger(x') \right]_\pm &= 0, \end{aligned} \quad (4)$$

where $i, j = \{+, -\}$.

For the harmonic potentials at hand, the Heisenberg equations of motion for the atomic field operators take the same form, independently of whether the atoms are bosonic or fermionic. It is convenient to expand them in terms of eigenstates $\{u_n(x)\}$ of one of the trap Hamiltonians H_\pm , say, H_+ for concreteness, as

$$\begin{aligned} \hat{\Psi}_+(x, t) &= \sum_n u_n(x) \hat{a}_n(t), \\ \hat{\Psi}_-(x, t) &= \sum_n u_n(x) \hat{b}_n(t), \end{aligned} \quad (5)$$

where the \hat{a}_n 's and \hat{b}_n 's satisfy either fermionic or bosonic commutation relations. In both cases, this expansion readily yields the Heisenberg equations of motion

$$\begin{aligned} i \frac{d\hat{a}_n}{d\tau} &= A_n \hat{a}_n + \tilde{g} \hat{b}_n, \\ i \frac{d\hat{b}_n}{d\tau} &= B_n \hat{b}_n + C_n \hat{b}_{n+2} + D_n \hat{b}_{n-2} + \tilde{g} \hat{a}_n, \end{aligned} \quad (6)$$

where we have introduced the coefficients

$$\begin{aligned} A_n &= \frac{1}{2} (\beta - 1) + n, \\ B_n &= \frac{1}{4} (\beta^2 - 1) (2n + 1) + n, \\ C_n &= \frac{1}{4} (\beta^2 - 1) \sqrt{(n + 2)(n + 1)}, \\ D_n &= \frac{1}{4} (\beta^2 - 1) \sqrt{n(n - 1)}, \end{aligned} \quad (7)$$

and the ratio

$$\beta = \omega_+ / \omega_- \quad (8)$$

of the trap frequencies. The dimensionless time τ is scaled to ω_+ , $\tau = \omega_+ t$, and so is the dimensionless coupling strength $\tilde{g} = g/\omega_+$.

We emphasize that while the operator \hat{a}_n describes the annihilation of atoms in level n of the upper trap, a similar interpretation of the \hat{b}_n 's is not possible, since they result from the expansion of the field operator of atoms in the internal state $|-\rangle$ on the basis of the “+”-trap. Denoting the eigenstates of the single-atom Hamiltonian of the lower trap as $\{v_n(x)\}$, the “true” annihilation operators \hat{c}_n associated with the trapped atoms in the $|-\rangle$ internal state are related to the \hat{b}_n 's by the mapping

$$\hat{c}_n(t) = \sum_n T_{nm} \hat{b}_m(t), \quad (9)$$

where the mapping matrix element T_{nm} is the overlap integral

$$T_{nm} = \int dx v_n(x) u_m(x). \quad (10)$$

III. DYNAMICS

In this section, we compare the dynamics of ideal non-interacting bosonic and fermionic systems evolving under the influence of the Raman coupling. We proceed by numerically solving the Heisenberg equations of motion (6) for a sample of N atoms initially in the internal state $|+\rangle$ and at temperature $T = 0$. For bosonic atoms, all atoms are therefore initially in the “+”-trap ground state, while for fermions they fill the lowest N trap levels. The corresponding initial states are correspondingly

$$|\psi_F(0)\rangle = \prod_{i=0}^{N-1} \hat{a}_i^\dagger |0\rangle_+ \otimes |0\rangle_-, \quad (11)$$

in the case of fermions and for bosonic atoms,

$$|\psi_B(0)\rangle = \frac{1}{\sqrt{N!}} \hat{a}_0^{\dagger N} |0\rangle_+ \otimes |0\rangle_- . \quad (12)$$

We consider, first, the case of noninteracting fermionic atoms. For trap frequencies approximately equal, $\beta \simeq 1$, Eq. (6) suggests the existence of two limiting situations, at least in the case of fermions. (We will revisit this point when discussing low-temperature bosonic systems.) In the first one, which we call the “strong-coupling regime” in the following, $\tilde{g} \approx N$, so that the inter-trap coupling dominates the dynamics and the intra-trap coupling terms $\hat{b}_{n\pm 2}$ can largely be ignored. In contrast, the “weak-coupling regime” $\tilde{g} \ll N$ is dominated by intra-trap coupling.

As a first measure of the system dynamics, Fig. 2 shows the difference

$$\begin{aligned} \Delta N(\tau) &= \frac{1}{N} \int dx \left[\langle \hat{\Psi}_+^\dagger(x) \hat{\Psi}_+(x) \rangle - \langle \hat{\Psi}_-^\dagger(x) \hat{\Psi}_-(x) \rangle \right] \\ &= \frac{1}{N} \sum_n \left(\langle \hat{a}_n^\dagger(\tau) \hat{a}_n(\tau) \rangle - \langle \hat{c}_n^\dagger(\tau) \hat{c}_n(\tau) \rangle \right) . \end{aligned} \quad (13)$$

between the populations of the “+” and “-” traps. Fig. 2a is for the strong-coupling regime, and 2b for the weak-coupling regime.

One can gain some intuitive understanding of the strong-coupling regime by remarking that in that regime, intra-trap transitions remain small, so that the Raman coupling is predominantly between levels of the two traps with equal quantum number n . To lowest order, these transitions are all at the Rabi frequency \tilde{g} . However, this simplest description cannot explain the result of Fig. 2a. Rather, it is necessary to include at least their lowest-order corrections, i.e.,

$$\Omega_n = \sqrt{g^2 + \frac{1}{4} (A_n - B_n)^2} \simeq \tilde{g} + \left(\frac{(\beta - 1)^2}{8\tilde{g}} \right) n^2 . \quad (14)$$

Such an n -dependence of Rabi frequencies is known to lead to collapse and revival phenomena, as was first discussed in the context of the Jaynes-Cummings model[7], where $\Omega_n \propto \sqrt{n}$. This is precisely the type of behavior exhibited by ΔN in the strong-coupling regime. Because of the n^2 -dependence of Ω_n , it is expected that the lowest trap levels play a dominant role in the appearance of the revivals. That this is indeed the case is confirmed numerically, and is illustrated in Fig. 3, which shows the level occupation of the “+”-trap for two different times. As a result of the n^2 dependence of Ω_n , the populations of the lowest trap levels oscillate more or less in phase, while those of higher n levels dephase rapidly. This figure also illustrates the weak excitation of levels above $n = N$.

We remark that both collapses and revivals of ΔN disappear when the two trap frequencies are identical, since for $\beta = 1$, we have $A_n = B_n = n$ and hence $\Omega_n = \tilde{g}$. In addition, intra-trap transitions vanish in that case, due to $C_n = D_n = 0$.

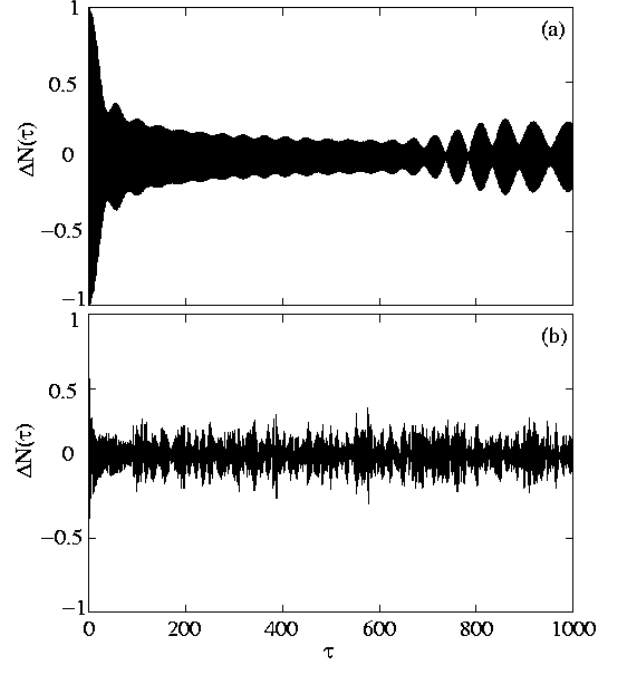


FIG. 2: $\Delta N(\tau)$ for $N = 35$ fermions and trap ratio $\beta = 0.9$, as obtained from a numerical integration of Eqs. (6): (a) strong coupling regime with $\tilde{g} = 31.0$; (b) weak coupling regime with $\tilde{g} = 2.0$.

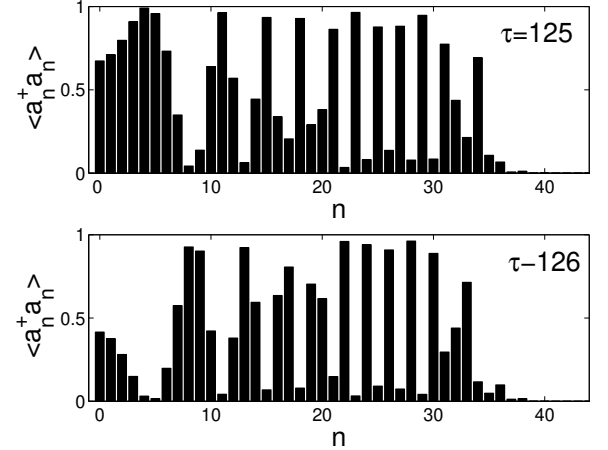


FIG. 3: Occupation of the upper trap levels at the dimensionless times $\tau = 125$ and 126 . Same parameters as in Fig. 2a.

Fig. 2b shows the inversion ΔN between the total trap populations in the weak-coupling regime, $\tilde{g} \ll N$. In this limit, inter-trap and intra-trap coupling occur on similar timescales. Immediately following a Raman transition from the $|+\rangle$ to the $|-\rangle$ internal state, the population of the “-”-trap starts to undergo a redistribution between its levels. The combined effects of the intra- and inter-trap

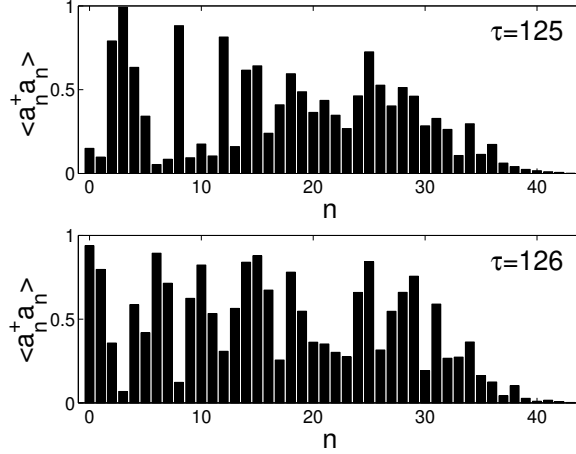


FIG. 4: Occupation of the upper trap at the two dimensionless times $\tau = 125, 126$ for the parameters of Fig. 2b.

transitions result in that case in a quasi-random evolution of $\Delta N(t)$ of Fig. 2b. Figure 4 shows the population of individual levels in the “+”-trap at two different times in this regime.

We now briefly turn to the case of a Bose gas. For a sample at zero-temperature and initially in the internal state $|+\rangle$, $T = 0$, all atoms are in the ground state of the “+”-trap at $t = 0$. As a result, the strong-coupling regime is characterized by almost perfect Rabi oscillations of the atomic population between the two trap ground states, with a small fraction of the atoms coupling to higher modes due to intra-trap transitions. This behavior is largely preserved in the (fermionic) weak coupling regime, provided that $\tilde{g} \gg \beta^2 - 1$. Indeed, Eqs. (6) show that in the $T = 0$ bosonic case, intra-trap coupling first occurs between the levels $n = 0$ and $n = 2$ of the “-”-trap, with coupling coefficient $D_2 = (\beta^2 - 1)/4$. As long as this coupling remains small compared to the inter-trap coupling \tilde{g} , the system acts effectively as a two-mode system. In other words, for low temperature bosonic systems, the weak-coupling regime is not characterized by $\tilde{g} \approx N$ as is the case for fermions, but rather by $\tilde{g} \ll \beta^2 - 1$.

IV. COLLISIONS

In this section, we discuss the effect of collisions on the preceding results. Collisions are of course central to the dynamics of quantum-degenerate atomic systems. They are essential in the evaporative cooling of the sample, and also provide a nonlinearity that can lead to the nonlinear mixing of matter waves. In bosonic systems, much new physics can be studied, e.g. by changing the sign of the scattering length characteristic of s -wave collisions. In the case of fermions the result in the creation of holes in the Fermi sea, and the filling of these holes by additional

collisions results in a heating that appears to fundamentally limit the temperatures at which these samples can be cooled. We discuss first the way collisions impact the operation of the Raman coupler in the case of fermions, and later compare these results with those for a bosonic sample.

It is well known that in fermionic atoms, the Pauli exclusion principle forbids the existence of s -wave scattering between atoms in the same internal state. In addition, p -wave scattering is generally negligible. Hence two-body collisions are described by the Hamiltonian

$$\hat{\mathcal{H}}_{\text{col}} = U_0 \int dx \hat{\Psi}_+^\dagger(x) \hat{\Psi}_-^\dagger(x) \hat{\Psi}_-(x) \hat{\Psi}_+(x), \quad (15)$$

where $U_0 = 4\pi\hbar^2 a\rho/m$ is the interaction strength with a being the s -wave scattering length and ρ the characteristic density of the system. Again, we expand the field operators according to Eq. (5) in terms of the basis $\{u_n\}$ and obtain

$$\hat{\mathcal{H}}_{\text{col}} = U_0 \sum_{i,j,k,l} U_{ijkl} \hat{a}_i^\dagger \hat{b}_j^\dagger \hat{b}_k \hat{a}_l, \quad (16)$$

where the matrix element

$$U_{ijkl} = \int dx u_i(x) u_j(x) u_k(x) u_l(x) \quad (17)$$

characterizes the scattering between different levels. We note that U_{ijkl} is symmetric under permutations.

In the presence of this quartic Hamiltonian, the Heisenberg equations of motion for the operators a_n and b_n involve cubic combinations of operators. To close this system of equations, we invoke a time-dependent Hartree-Fock ansatz to factorize products of operators, of the generic form $\hat{b}_i^\dagger(t) \hat{b}_j(t) \hat{a}_k(t)$, by

$$\hat{b}_i^\dagger(t) \hat{b}_j(t) \hat{a}_k(t) \approx \langle \hat{b}_i^\dagger(t) \hat{b}_j(t) \rangle \hat{a}_k(t) - \langle \hat{b}_i^\dagger(t) \hat{a}_k(t) \rangle \hat{b}_j(t), \quad (18)$$

where the expectation value is over the state $|\psi_F(0)\rangle$ since we work in the Heisenberg picture. At this level of approximation, we neglect all contributions from pairing. This factorization scheme readily yields the time-dependent Hartree-Fock equations of motion (in dimensionless variables)

$$\begin{aligned} i \frac{\partial \hat{a}_n}{\partial \tau} &= \sum_k \left[(A_n \delta_{nk} + Q_{nk}^{bb}) \hat{a}_k - \left(Q_{nk}^{ab*} - \tilde{g} \delta_{nk} \right) \hat{b}_k \right] \\ i \frac{\partial \hat{b}_n}{\partial \tau} &= \sum_k \left[(B_n \delta_{nk} + Q_{nk}^{aa}) \hat{b}_k - \left(Q_{nk}^{ab} - \tilde{g} \delta_{nk} \right) \hat{a}_k \right] \\ &+ C_n \hat{b}_{n+2} + D_n \hat{b}_{n-2}, \end{aligned} \quad (19)$$

where we have introduced the time-dependent coefficients

$$\begin{aligned} Q_{nk}^{aa}(\tau) &= \tilde{U}_0 \sum_{i,j} U_{n,i,j,k} \langle \hat{a}_i^\dagger(\tau) \hat{a}_j(\tau) \rangle \\ Q_{nk}^{bb}(\tau) &= \tilde{U}_0 \sum_{i,j} U_{n,i,j,k} \langle \hat{b}_i^\dagger(\tau) \hat{b}_j(\tau) \rangle \\ Q_{nk}^{ab}(\tau) &= \tilde{U}_0 \sum_{i,j} U_{n,i,j,k} \langle \hat{a}_i^\dagger(\tau) \hat{b}_j(\tau) \rangle, \end{aligned} \quad (20)$$

and $\tilde{U}_0 = U_0/\hbar\omega_+$ is a dimensionless interaction strength.

The effect of collisions is illustrated in Figs. 5b,c, which show the population inversion $\Delta N(\tau)$ for two values of the interaction strength \tilde{U}_0 . Figure 5a shows the collisionless case for reference.

For weak enough collisions, the dynamics of the system is not significantly altered, as should of course be expected. However, we observe a quantitative change is the dynamics of ΔN as \tilde{U}_0 is further increased. Instead of a collapse and revivals, $\Delta N(\tau)$ now undergoes nearly full Rabi oscillations.

A first hint at the cause of this changed behavior is offered by Fig. 6, which shows a snapshot of the level populations in the “+”-trap for the cases of Fig. 5a and 5b, respectively. We observe that the smaller value of \tilde{U}_0 corresponds to an inhomogeneous level population distribution, whereas the higher nonlinearity causes the trap levels to be almost equally populated.

A more quantitative understanding of the role of collisions can be gained by estimating how the nonlinear terms in Eq. (19) modify the (collisionless) Rabi frequency. A numerical evaluation of the coefficients U_{ijkl} shows that elastic collisions, $i = j = k = l$, dominate the dynamics of the system. In addition, U_{nnnn} turns out to be a decreasing function of n . Keeping the elastic contributions to the collision-induced dynamics only, and neglecting as in the strong-coupling regime of section III the effects of intra-trap coupling terms $\hat{b}_{n\pm 2}$, one find that Eq. (14) is approximately changed to

$$\Omega_n^{NL}(\tau) = \sqrt{g^2 + \frac{1}{4} (A_n - B_n + Q_{nn}^{bb}(\tau) - Q_{nn}^{aa}(\tau))^2}. \quad (21)$$

Fig. 7 shows, as a function of \tilde{U}_0 , the time-dependent Rabi frequencies $\Omega_n^{NL}(\tau)$ averaged over a time interval Θ large compared to their inverse,

$$\bar{\Omega}_n = \frac{1}{\Theta} \int_0^\Theta d\tau \Omega_n^{NL}(\tau). \quad (22)$$

Because U_{nnnn} is a decreasing function of n , its contribution tends to compensate the n^2 dependence of Eq. (14). As a result, there is a range of collisions strengths for which the dependence of $\Omega_n^{NL}(\tau)$ on n largely disappears. In this range, paradoxically, the dynamics of the collision-dominated Fermi system resembles that of a collisionless Bose system. From this admittedly crude argument — which is however consistent with our full numerical results — we also conjecture that for even larger \tilde{U}_0 , the approximate cancellation of the n -dependence of the Rabi frequencies will disappear and we expect an overall dephasing and decay of the population difference $\Delta N(t)$. It has unfortunately proven prohibitive to try and check this conjecture numerically.

We now turn to the case of bosonic atoms. Bose statistics allows for s -wave collisions between atoms in the same spin state, so that the collisional Hamiltonian is

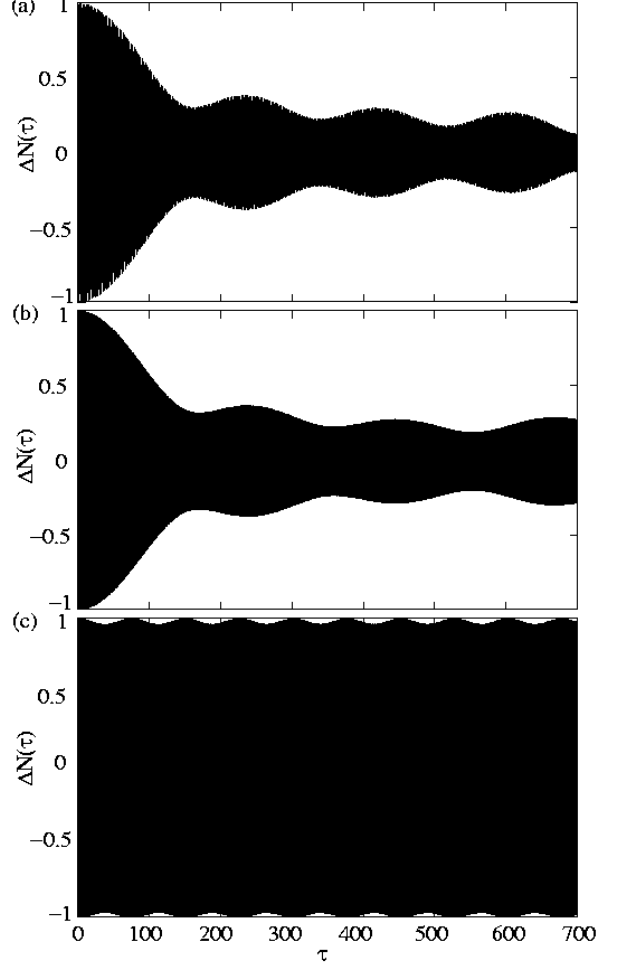


FIG. 5: Population difference $\Delta N(\tau)$ for $N = 10$ fermions, a trap ratio $\beta = 0.9$ and in the strong-coupling regime $\tilde{g} = 10.0$. The plots, which result from the numerical integration of Eqs. (19), are for different strengths of the two-body collisions: (a) $\tilde{U}_0 = 0.0$; (b) $\tilde{U}_0 = 0.01$; (c) $\tilde{U}_0 = 0.1$.

now

$$\begin{aligned} \hat{\mathcal{H}}_{\text{col}} = & U_+ \int dx \hat{\Psi}_+^\dagger(x) \hat{\Psi}_+^\dagger(x) \hat{\Psi}_+(x) \hat{\Psi}_+(x) \\ & + U_- \int dx \hat{\Psi}_-^\dagger(x) \hat{\Psi}_-^\dagger(x) \hat{\Psi}_-(x) \hat{\Psi}_-(x) \\ & + 2U_x \int dx \hat{\Psi}_+^\dagger(x) \hat{\Psi}_-^\dagger(x) \hat{\Psi}_+(x) \hat{\Psi}_-(x), \end{aligned} \quad (23)$$

where the U_i , $i = +, -, x$, characterize the strength of the collisions. In the following we assume for simplicity $U_+ = U_- = U_0$ and $U_x = \eta_x U_0$.

To truncate the Heisenberg equations of motion for the field operators, we now invoke a mean-field approximation, factorize all products of operators, and replace the resulting expectation values by time-dependent c -

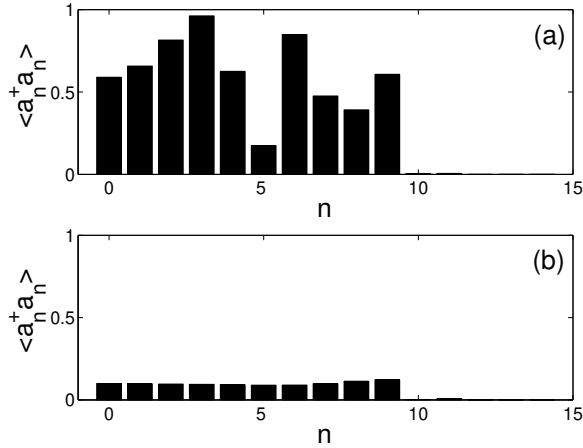


FIG. 6: Occupation of the upper trap at $\tau = 490$: (a) for the parameters of Fig. 5(b) and (b) for the parameters of Fig. 5(c).

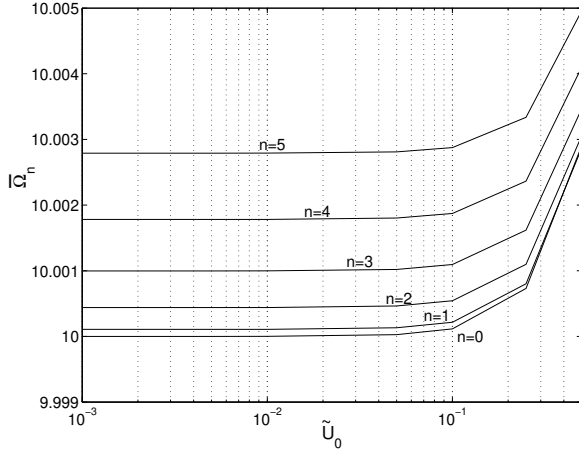


FIG. 7: Semi-logarithmic plot of the time-averaged generalized Rabi frequencies for the six lowest trap levels as a function of the nonlinear parameter, otherwise the same parameters as in Fig. 5 are used.

numbers. This gives

$$\begin{aligned} i \frac{d\langle \hat{a}_n \rangle}{d\tau} &= \sum_k (A_n \delta_{nk} + Q_{nk}^{aa} + \eta_x Q_{nk}^{bb}) \langle \hat{a}_k \rangle + \tilde{g} \langle \hat{b}_n \rangle \\ i \frac{d\langle \hat{b}_n \rangle}{d\tau} &= \sum_k (B_n \delta_{nk} + Q_{nk}^{bb} + \eta_x Q_{nk}^{aa}) \langle \hat{b}_k \rangle + \tilde{g} \langle \hat{a}_n \rangle \\ &+ C_n \langle \hat{b}_{n+2} \rangle + D_n \langle \hat{b}_{n-2} \rangle, \end{aligned} \quad (24)$$

where

$$Q_{nk}^{aa}(\tau) = 2\tilde{U}_0 \sum_{i,j} U_{n,i,j,k} \langle \hat{a}_i(\tau) \rangle^* \langle \hat{a}_j(\tau) \rangle$$

$$Q_{nk}^{bb}(\tau) = 2\tilde{U}_0 \sum_{i,j} U_{n,i,j,k} \langle \hat{b}_i(\tau) \rangle^* \langle \hat{b}_j(\tau) \rangle, \quad (25)$$

and the expectation values are with respect to the state $|\psi_B(0)\rangle$. Figure 8 shows the inversion $\Delta N(t)$ for a sample of bosonic atoms initially in the internal state $|+\rangle$. Fig. 8a, which is for $\tilde{U}_0 = 0.1$, is practically indistinguishable from the collisionless situation. It exhibits full Rabi oscillations indicating that only one mode is significantly populated in each of the “+”- and “-”-trap. As the strength of collisions is increased, however, one starts observing a damping of the oscillations, see Fig. 8b. This is clearly a result of the scattering of atoms into higher trap states. The transitions between these states are characterized by n -dependent Rabi-frequencies, leading to the onset of a dephasing process resembling the situation for noninteracting fermions [8].

It is known from nonlinear optics [9] and atom optics [10] that systems governed by a pair of coupled nonlinear Schrödinger equations can reach a regime where the nonlinear phase shifts dominate their dynamics. Such two-mode systems exhibit Rabi oscillations for small nonlinearities, but mode-coupling is inhibited above a certain strength of the nonlinearity. We have not observed this effect in the present multimode system, a result of the strong inter-mode scattering. However, we can recover this behavior if we artificially set all but the diagonal elements of U_{ijkl} equal to zero, i.e. if we keep only elastic scattering. The Raman coupler then becomes effectively a two-mode system described by the exactly solvable equations of the nonlinear coupler

$$\begin{aligned} i \frac{d\langle \hat{a}_0 \rangle}{d\tau} &= \frac{1}{2}(\beta - 1) \langle \hat{a}_0 \rangle + \tilde{g} \langle \hat{b}_0 \rangle \\ &+ Q \left(|\langle \hat{a}_0 \rangle|^2 + \eta_x |\langle \hat{b}_0 \rangle|^2 \right) \langle \hat{a}_0 \rangle \end{aligned} \quad (26)$$

$$\begin{aligned} i \frac{d\langle \hat{b}_0 \rangle}{d\tau} &= \frac{1}{4}(\beta^2 - 1) \langle \hat{b}_0 \rangle + \tilde{g} \langle \hat{a}_0 \rangle \\ &+ Q \left(|\langle \hat{b}_0 \rangle|^2 + \eta_x |\langle \hat{a}_0 \rangle|^2 \right) \langle \hat{b}_0 \rangle, \end{aligned} \quad (27)$$

with $Q = 2\tilde{U}_0 U_{0000}$. The critical interaction strength \tilde{U}_c [11] above which mode coupling becomes inhibited is known to be

$$\tilde{U}_c = \frac{2\tilde{g}}{NU_{0000}(\eta - \eta_x)}. \quad (28)$$

Figure 9 shows the nonlinear switching behavior of this model system for values of the nonlinearity above and below this critical value. Clearly, this is very different from the dynamics of the full multimode system of Fig. 8.

We see, then, that in the case of interacting bosons, intra-trap scattering is an important element of the dynamics of the Raman coupler, and the system rapidly evolves to a multimode behavior; in contrast in the fermionic case U_{ijkl} tends to reduce the spread in Rabi frequencies and thus inhibits dephasing.

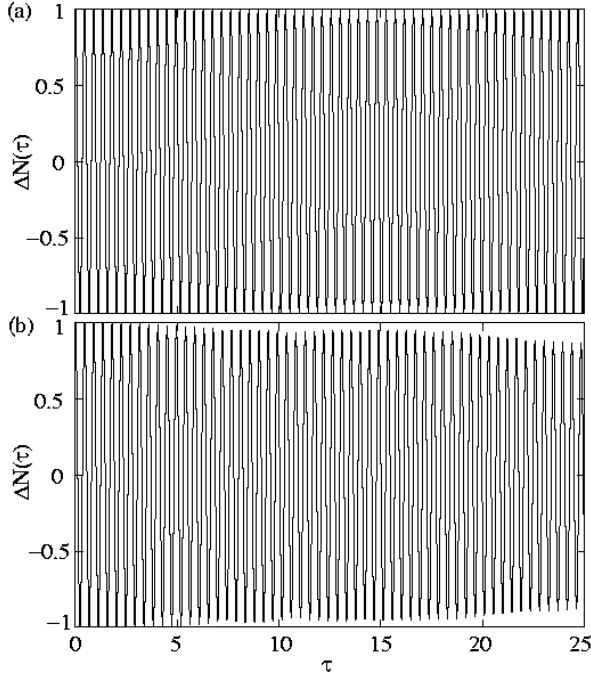


FIG. 8: $\Delta N(\tau)$ for $N = 20$ bosons, trap ratio $\beta = 0.9$, linear coupling $\tilde{g} = 7.0$ and the cross interaction parameter $\eta_x = 0.5$. Shown is the full simulation of Eq. (24) with (a) $U_0 = 0.1$ and (b) $\tilde{U}_0 = 0.5$.

V. SUMMARY

The Raman coupling between two internal states of a trapped Fermi gas exhibits a rich dynamics, quite different from its bosonic counterpart. This is of course due primarily to the fact that a Fermi gas occupies a large number of trap states, and hence can never be approximated as a two-mode system. In particular, we have identified two limiting regimes, dependent upon whether inter-trap or intra-trap dynamics is dominant. In the general situation where the traps associated with the two internal states have different frequencies, the first of these regimes leads to dynamics characterized by collapses and revivals. However, two-body collisions can under appropriate conditions inhibit this behavior, making the collision-dominated Fermi system more similar to a collisionless Bose system. In this regime, there is an interesting parallel between collision-dominated Fermi systems and collisionless Bose systems, and conversely.

The numerical analysis of fermionic systems appears to be presently limited to very small numbers N of atoms, a result of the large memory requirements associated with the need to keep track of a large number of quantum states. Indeed, most of our numerical results are limited to N less than or of the order of 35, and even this required rather large computing facilities. Despite this limitation and its associated lack of quantitative predic-

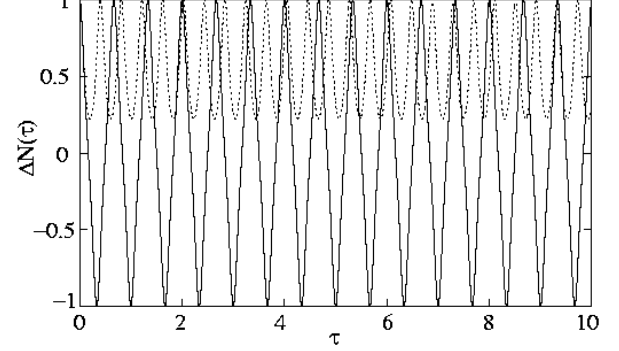


FIG. 9: $\Delta N(\tau)$ for $N = 20$ bosons, trap ratio $\beta = 0.9$, linear coupling $\tilde{g} = 7.0$ and the cross interaction parameters $\eta_x = 0.5$. We assumed that only the diagonal elements U_{nnnn} in Eq. (24) contribute and set all others to zero. We have $U_{0000} \approx 0.40$, so that the critical value of the nonlinearity is $\tilde{U}_c \approx 3.5$. We show plots for $\tilde{U}_0 = 3.2 < \tilde{U}_c$ (solid) and $\tilde{U}_0 = 3.6 > \tilde{U}_c$ (dotted).

tions, our analysis sheds useful light on the dynamics of trapped Fermi systems, in particular in the presence of collisions, and will provide useful guidance in understanding more realistic trapped Fermi gases in three dimensions and with a large number of fermionic atoms.

Acknowledgments

We thank J. V. Moloney for providing us with CPU time on his parallel cluster, and E. M. Wright and C. P. Search for valuable discussions. This work is supported in part by the US Office of Naval Research under Contract No. 14-91-J1205, by the National Science Foundation under Grant No. PHY-0098129, by the US Army Research Office, by NASA, and by the Joint Services Optics Program.

-
- [1] B. DeMarco and D. S. Jin, *Science* **285**, 1703 (1999); A. G. Truscott *et al.*, *Science* **291**, 2570 (2001); B. DeMarco *et al.*, *Phys. Rev. Lett.* **86**, 5409 (2001); F. Schreck *et al.*, *Phys. Rev. Lett.* **87**, 080403 (2001).
[2] H. T. C. Stoof *et al.*, *Phys. Rev. Lett.* **76**, 10 (1996); M.

- Houbiers *et al.*, *Phys. Rev. A* **56**, 4864 (1997); G. Bruun *et al.*, *Eur. Phys. J. D* **7**, 433 (1999); L. You and M. Marinescu, *Phys. Rev. A* **60**, 2324 (1999); M. A. Baranov, *JETP Lett.* **64**, 301 (1996); E. Timmermans *et al.*, *Phys. Lett. A* **285**, 228 (2001); E. Holland *et al.*, *Phys.*

- Rev. Lett. **87**, 120406 (2001).
- [3] M. H. Anderson *et al.*, Science **269**, 198 (1995); K. B. Davis *et al.*, Phys. Rev. Lett. **75**, 3969 (1995); C. C. Bradley *et al.*, Phys. Rev. Lett. **75**, 1687 (1995).
- [4] E. Timmermans, Phys. Rev. Lett. **87**, 240403 (2001).
- [5] P. Meystre, *Atom Optics* (Springer-Verlag, New York, 2001).
- [6] M. O. Mewes, M. R. Andrews, D. M. Kurn, D. S. Durfee, C. G. Townsend, and W. Ketterle, Phys. Rev. Lett. **78**, 582 (1997); E. W. Hagley, L. Deng, M. Kozuma, J. Wen, K. Helmerson, S. L. Rolston, W. D. Phillips, Science **283**, 1706 (1999); I. Bloch, T. W. Hänsch, and T. Esslinger, Phys. Rev. Lett. **82**, 3008 (1999).
- [7] , F. W. Cummings, Phys. Rev. **140**, A1051 (1965).
- [8] We were not able to simulate longer times, because numerically we had to work with a finite number of modes and the scattering process started populating modes close to our chosen numerical cut-off.
- [9] S. M. Jensen, IEEE Journal of Quantum Electronics **QE-18**, 1580 (1982).
- [10] K. J. Schermann, G. Lenz, and P. Meystre, Phys. Rev. A **51**, 3121 (1995).
- [11] Usually, the nonlinear switching behavior is given by a critical intensity or atom number. Since we assume to vary the interaction strength, we fix the number of atoms and define a critical nonlinearity to be consistent in our approach.